Analyst

PAPER

View Article Online
View Journal

Cite this: DOI: 10.1039/c4an00897a

Prussian blue–Au nanocomposites actuated hemin/G-quadruplexes catalysis for amplified detection of DNA, Hg^{2+} and adenosine triphosphate†

Guangfeng Wang,*[ab] Ling Chen,[ab] Yanhong Zhu,[ab] Xiuping He,[ab] Gang Xu[ab] and Xiaojun Zhang*[ab]

In this paper, horseradish peroxidase-mimicking DNAzyme (HRP-DNAzyme) and Prussian blue (PB)–gold (Au) nanocomposites were designed as versatile electrochemical sensing platforms for the amplified detection of DNA, Hg^{2+} and adenosine triphosphate (ATP). By the conjugation of the target probe with the capture probe, a conformational change resulted in the formation of HRP-DNAzyme on the PB–Au modified electrode. The redox of HRP-DNAzyme (red) was efficiently carried out in the presence of H_2O_2, in which PB acted as a mediator stimulating the biocatalytic functions of HRP-DNAzyme and actuated a catalytic cycle bringing an amplified signal. Specific recognition of the target DNA, Hg^{2+} and ATP allowed selective amperometric detection of the target molecule. The detection limits of DNA, Hg^{2+} and ATP were 50 nM, 30 pM and 3 nM, respectively. The highlight of this work is that the catalytic cycle between PB–Au nanocomposites and HRP-DNAzyme was adequately utilized in the amplification platform for versatile sensing. The novel electrocatalytic biosensor involving only one-step incubation exhibited a wide linear range, low detection limit, and satisfactory selectivity and operational stability. The proposed approach provided an ease-of-use and universal reporting system with a simple design and easy operations.

Received 18th May 2014
Accepted 29th July 2014

DOI: 10.1039/c4an00897a

www.rsc.org/analyst

1. Introduction

With the progress in genomics and the Human Genome Project, nucleic acid-based sensors have become a booming field over the past 20–30 years because of their attractive features, such as high sensitivity, fast response and cost-effective requirements,[1,2] which is needed both for preventative therapy of genetic disorders, prognosis of cancer and postcytotoxic therapy, and for the treatment of bacterial and viral infections.[3] Electrochemical nucleic acid-based sensors involve the analysis of DNA,[2,4] the detection of aptamer-substrate complexes,[5] the sensing of metal ions[6] and so on. As we know, the amplification of recognition events is a central element in analytical or bioanalytical science.[7,8] Great efforts have also been made to develop signal amplified electrochemical DNA based sensors.[9] In DNA-based sensors, the signal amplification is usually achieved with various surface modifications[10] or by attaching additional labels to DNA, such as enzymes,[11] liposomes,[12] quantum dots,[13] or metal nanoparticles,[14] which may have a considerable effect on the resulting response. Among the various ingenious strategies available, signal amplification involving enzyme labels have received particular attention in electrochemical DNA-based sensor due to the intrinsic signal amplification provided by biocatalytic reactions.[15] Numerous sensor configurations for the amplified detection of DNA[2,10,16,17] or aptamer substrate complexes[18] were reported using protein enzymes as amplifying labels. However, the major obstacle of this strategy is the cumbersome enzyme labelling process, spatial distribution and producing substrate loss of the acting enzyme. In addition, conventional enzymes, such as horseradish peroxidase, glucose oxidase *etc.*, usually induce complicated synthesis, poor thermal stability and easily specific adsorption, thereby limiting their use as reporters for bioanalytical applications to a large extent. Moreover, biocatalytic amplification of an enzyme alone with poor substrate uptake rates largely influences the sensitivity.[19,20] Thus, adopting new designs to solve these problems is beneficial for the signal amplification in an electrochemical DNA-based sensor.

Recently, catalytic nucleic acids (DNAzymes) have become the focus of amplifying units for the detection of DNA[21] or

[a]*Key Laboratory of Chem-Biosensing, Key Laboratory of Functional Molecular Solids, College of Chemistry and Materials Science, Center for Nano Science and Technology, Anhui Normal University, Wuhu 241000, Anhui, PR China*

[b]*State Key Laboratory of Chemo/Biosensing and Chemometrics, Hunan University, Changsha 410082, PR China. E-mail: xjzhang@mail.ahnu.edu.cn; wangyuz@mail.ahnu.edu.cn*

† Electronic supplementary information (ESI) available. See DOI: 10.1039/c4an00897a

aptamer-substrate complexes,[22,23] and so on. Horseradish-peroxidase-mimicking DNAzyme (HRP-DNAzyme), a complex with hemin into a single-stranded guanine-rich aptamer to stack as a G-quadruplex nucleic acid structure, is one of the most explored DNAzymes,[24,25] which can effectively catalyze the H_2O_2-mediated oxidation of 2,2-azinobis(3-ethylbenzothiozoline)-6-sulfonic acid,[26,27] luminol,[28,29] 3,3′,5,5′-tetramethylbenzidine[30,31] *etc.* It has been applied in the sensing of DNA,[21,23,32] proteins,[22,33] or metal ions[34,35] with less expense and higher thermal stability compared to natural proteinogenic enzymes. Willner *et al.* reported nucleic acid based "machines" that generate the HRP-DNAzyme revealing its bioelectrocatalytic functions.[1] HRP-DNAzyme acting as peroxidase-like complexes in electrochemical DNA-based sensor, avoiding the fussy labeling process, provides an ideal candidate for the development of a sensitive and simple bioanalytical platform. Besides its peroxidase-like catalytic character, HRP-DNAzyme has also been researched[36,37] with other amplified strategies, including recycling[36] or accumulating[37] the reaction. Meanwhile, it is also a preferable method to amplify the signal of biosensors by employing an electron transfer mediator, such as ferrocene derivatives,[38] methylene blue[39] and meldola blue.[40] However, up to now, there are few reports of a signal amplification strategy based on the HRP-DNAzyme in company with the electron mediator.[41]

Prussian blue (PB) or iron(III) hexacyanoferrates(II), are characterized by fast dynamics of charge propagation. Although they are often demonstrated to act as powerful electrocatalysts for the reduction of hydrogen peroxide,[42] it also possesses another important role as electron mediator owing to its capability to provide electrical contact or a pathway for electron transfer.[43]

Inspired by the bioelectrocatalytic functions of the HRP-DNAzyme and the excellent electron mediator property of PB, we constructed a new electrochemical biosensor based on the catalysis cycle between HRP-DNAzyme and PB for the detection of DNA, Hg^{2+} and ATP. The aim of this work is to fabricate an ease-of-use and universal signal amplified reporting system to detect DNA-relative biomolecules.

2. Experimental section

2.1 Materials and apparatus

HPLC-purified oligonucleotides (sequences are listed in Table S1, ESI†) were obtained from Sangon Biotechnology Co. Ltd (Shanghai, China). The oligonucleotides were used as provided and diluted in pH 7.4, 20 mM Tris–HCl buffer solution (containing 100 mM NaCl, 20 mM KCl and 2 mM $MgCl_2$) to give stock solutions with the concentration of 10 μM. Each oligonucleotide was heated to 95 °C for 10 min, and then cooled slowly to 30 °C to remove aggregates. Chloroauric acid ($HAuCl_4 \cdot 4H_2O$), potassium ferricyanide ($K_3Fe(CN)_6$) and other reagents were also obtained from the Sinopharm Chemical Reagent Co. Ltd. (Shanghai, China). Ultrapure water (18.2 MΩ cm) was purified with PSDK2-10-C (Beijing, China) and used throughout the experiments. The basic composition of hybridization buffer was 0.05 M PBS buffer (pH = 7.4) and 100 mM $NaNO_3$. The pH of PBS was measured with a glass electrode connected to a PHS-3C pH meter (Shanghai, China). Centrifugation was performed using a HERMLEZ 36 HK apparatus (Wehingen, Germany). Electrochemical measurements were conducted on CHI 660 electrochemical analyzers (CH Instruments), which was controlled by a personal computer with a saturated calomel electrode (SCE) as the reference electrode, a glassy carbon electrode (GCE) as the working electrode, and platinum wire as the auxiliary electrode. Scanning electron microscopy (SEM) images of the prepared composites were obtained using Hitachi S-4800 SEM (operated at 10 kV).

2.2 Modification of the electrode with PB–Au nanocomposites

GCE was used for preparing the biosensor in this paper. First, GCE was carefully polished with alumina slurry (0.3 mm and 0.05 mm, respectively). Immediately after, GCE was rinsed and sonicated in ethanol and ultrapure water for 3 min each, removing the alumina residue from the electrode surface. The prepared electrode was dried under a flowing nitrogen atmosphere. For the modification of PB–Au nanocomposites films, potassium ferricyanide (1 mM) and equimolar chloroauric acid contained in a solution of 0.1 M KNO_3 with 0.05 M PBS (pH 3.2) were prepared for electrodeposition.[44] The potential range of electrodeposition was from 0.0 to 1.0 V and the scan rate was 50 mV s^{-1}. After 20 potential cycles, the PB–Au nanocomposites films were formed on GCE, which was then named as PB–Au/GCE. As the control experiment, Au nanoparticles modified glassy carbon electrode (Au/GCE) was also prepared, and electrodeposition was carried out in 1 mg mL^{-1} chloroauric acid at −0.2 V for 20 s.

2.3 Self-assembly of capture probe on PB–Au/GCE

The immobilization of the capture probe, S1, was performed by dropping 30 μL of 0.05 M PBS buffer (pH 7.4) containing 1.0 μM S1 probe and 0.4 M NaCl on the PB–Au/GCE in a humidified chamber. The self-assembly through the thiol of S1 and Au atom was proceeded for 10 h. GCE was then rinsed with water and incubated in 2 mM 6-mercaptohexanol in PBS buffer (0.05 M, pH 7.4) for 2 hours to eliminate the nonspecific-bonded DNA.[45]

2.4 Detection of DNA, Hg^{2+} and ATP

For the further modification of hemin/G-quadruplex on PB–Au nanocomposites-modified GCE, the S1/PB–Au/GCE electrodes were then incubated with 3 μM S2, 0.2 mM hemin and K^+ in the hybridization buffer solution at 37 °C for 10 h to form HRP-DNAzyme, which was then defined as HRP-DNAzyme/S1/PB–Au/GCE.

For the detection of target DNA sequence (S2), series concentrations of S2 were used to incubate with the S1/PB–Au/GCE. For the control experiment, S3 (matching with S1 but without G-rich) was substituted S2 under the same conditions of the above to prepare the modified electrode without the HRP-DNAzyme structure (No HRP-DNAzyme/S1/PB–Au/GCE).

For the detection of Hg^{2+}, 3.0 μM S4 [sequence designed with thymines at the 3′ end for matching with S1 in the presence of

Hg^{2+} by 9 specific thymine–Hg^{2+}–thymine (T–Hg^{2+}–T) base pairs] was used to hybridize with S1/PB–Au/GCE for 10 h in the hybridization buffer containing 0.2 mM hemin, K^+ and different concentrations of Hg^{2+}, which was the same condition as that for the preparation of HRP-DNAzyme/S1/PB–Au/GCE. HRP-DNAzyme and PB–Au nanocomposites-based Hg^{2+} biosensor was prepared and named as Hg^{2+}–HRP-DNAzyme/S1/PB–Au/GCE.

For the detection of ATP under the same conditions, S5 and S6 (the aptamer of ATP) substituted for S1 and S2, respectively. The immobilization of the capture probe (S5) was performed by dropping 30 μL of PBS buffer containing 1.0 μM S5 probe on the cleaned GCE. S5 was then self-assembled on the PB–Au/GCE electrode after incubating for 10 h named as S5/PB–Au/GE. The modified electrode was rinsed and repeated with the same experimental process as that of S1/PB–Au/GE to eliminate the nonspecific-bonded DNA. S5/PB–Au/GE was then incubated with different concentrations of ATP and 3.0 μM S6 in the hybridization buffer for 10 h to prepare the ATP biosensors (ATP–HRP-DNAzyme/S5/PB–Au/GCE). When the assembly was complete, all the modified electrodes were thoroughly rinsed and dried with N_2 before electrochemical measurements.

2.5 Electrochemical assay

Cyclic voltammetry (CV) was performed in 0.05 M PBS (pH 7.4) or containing 200 μM H_2O_2 within the potential range from 0.6 to −0.2 V at a scan rate of 50 mV s^{-1}. Electrochemical impedance spectroscopy (EIS) was performed in PBS (0.05 M, pH 7.4) containing 5 mM $Fe(CN)_6^{3-}$/$Fe(CN)_6^{4-}$ and 0.1 M KCl in the frequency range from 0.1 Hz to 100 kHz with 5 mV as the amplitude at a polarization potential of −0.18 V. An amperometric current was also conducted at −0.2 V in PBS (0.05 M, pH 7.4) with the addition of H_2O_2 as the solution was stirred at 3000 rpm for optimal sensitivity. All the electrochemical experiments were carried out at room temperature.

3. Results and discussion

3.1 Strategy of the assay

Scheme 1 illustrates the fabrication of the amplified DNA sensors. As shown, the PB–Au nanocomposites were first modified onto the surface of GCE by electrochemical deposition. The capture probe, S1, was then assembled on the PB–Au/GCE due to the strong chemical bond of Au–S. The target DNA probe, S2 was ingeniously designed with two sections. Section I was complementary to the 9 bases at 3′ end of S1, and another section of it, section II, was a G-rich sequence, which can form a HRP-DNAzyme structure in the presence of K^+ and hemin. Thus, after the target DNA was captured by the immobilized S1 through the complementary base pairs, in the presence of K^+ and hemin, the G-rich sequence was stacked as a G-quadruplex–hemin complex, and HRP-DNAzyme was assembled near the electrode forming HRP-DNAzyme/S1/PB–Au/GCE. Because of the biocatalytic character of the peroxidase-like complex HRP-DNAzyme,[19] in the presence of H_2O_2, a catalytic cycle may occur with PB. First, under an applied potential, PB was reduced to

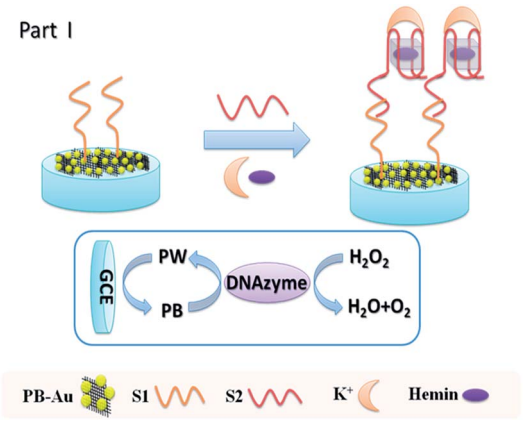

Scheme 1 Fabrication process of the electrochemical amplified determination of S2 based on PB–Au nanocomposites actuated HRP-DNAzyme system.

PW (Prussian white) near the electrode transferring electrons from the surface of the electrode.[46] The resulting PW was then oxidized back to PB by HRP-DNAzyme (ox), which itself was reduced to HRP-DNAzyme (red). HRP-DNAzyme (red) was oxidized to HRP-DNAzyme (ox) for further cycling by H_2O_2 with the product of H_2O. Thus, PB played a role of electron mediator in the system and there existed a catalytic recycle of PB and HRP-DNAzyme, as Scheme 1 shows, resulting in an amplification of the electrochemical signal. The process of PB–Au nanocomposites and HRP-DNAzyme based catalytic cycle is summarized by the following equations.

$$\text{Prussian blue (PB)} + e^- \rightarrow \text{Prussian white (PW)}$$

$$\text{HRP-DNAzyme (red)} + H_2O_2 \rightarrow \text{HRP-DNAzyme (ox)} + H_2O + O_2$$

$$\text{HRP-DNAzyme (ox)} + \text{Prussian white (PW)} \rightarrow \text{HRP-DNAzyme (red)} + \text{Prussian blue (PB)}$$

3.2 SEM, EIS and CV characterization

SEM images of Au nanoparticles (A) and PB–Au nanocomposites (B) electrodeposited on GCE are shown in Fig. 1. From Fig. 1A, we could see clearly that Au nanoparticles were successfully synthesized by electrodeposition. Compared with the SEM image of Au nanoparticles, it was obviously noticed that different from the SEM image of Au nanoparticles, on the surface of Au nanoparticles there appeared some specific PB nanostructure as labeled in the inset in Fig. 1B, in the SEM image of PB–Au nanocomposites. Electrochemical impedance is an effective method for probing the features of surface-modified electrodes, EIS was performed to study the different interfacial processes of the modified electrodes. As shown in Fig. 1C (curve a), the impedance spectrum of the bare GCE included a very small semicircle domain. When the electrode was modified with PB–Au nanocomposites (curve b), there was almost no semicircle, illustrating the good electron transfer nature of

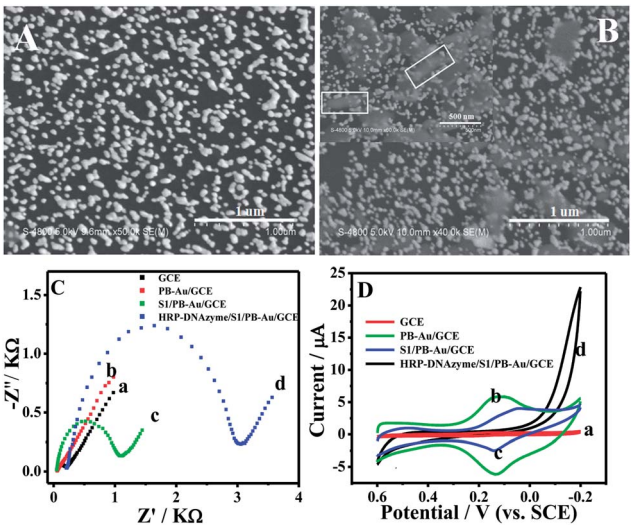

Fig. 1 SEM images of Au nanoparticles (A) and PB–Au (B) nanocomposites with the high magnification of SEM image in the inset; (C) Nyquist plot for EIS measurements of different electrodes: bare GCE (a), PB–Au/GCE (b), S1/PB–Au/GCE (c), HRP-DNAzyme/S1/PB–Au/GCE (d); (D) CV of different electrodes in 0.05 M PBS (pH 7.4) containing 200 μM H_2O_2: bare GCE (a), PB–Au/GCE (b), S1/PB–Au/GCE (c), HRP-DNAzyme/S1/PB–Au/GCE (d) (0.95 μM S2 as example).

PB–Au nanocomposites. After the immobilization of S1, a semicircle could be observed due to the formation of a negatively charged interface, which may electrostatically repel negatively charged redox species $[Fe(CN)_6]^{3-}/^{4-}$ (curve c). When the electrode was further hybridized with S2, the diameter of the semicircle continued to increase (curve d), indicating the further loading of negatively charged DNA strands. All these impedance spectra were coherent as predicted. To prove our design, CVs at each immobilization step were also recorded to monitor the fabrication of the proposed biosensor. As shown in Fig. 1D, the bare GCE (curve a) showed no redox peak, but on either of the PB–Au/GCE (curve b) and S1/PB–Au/GCE (curve c), there appeared a pair of redox peaks at about 0.18 V from PB, which further proved the existence of PB. All these three electrodes showed weak electrochemical response towards H_2O_2 at −0.2 V. However, HPR-DNAzyme/S1/PB–Au/GCE, showed an obvious response towards H_2O_2 (curve d) at −0.2 V. We suggested the signal amplification probably result from the catalytic cycling of PB and hemin/G-quadruplexes. In a control experiment, the effect of PB and HRP-DNAzyme for the electrochemical amplification were investigated and discussed (the details were shown as Fig. S1 in ESI†), it proved that HRP-DNAzyme was also very important for constructing the electrochemical catalytic cycle with PB.

3.3 Electrochemical catalysis on H_2O_2

Because the HRP-DNAzyme/S1/PB–Au/GCE had an obvious electrochemical catalysis effect on H_2O_2, we studied a series of H_2O_2 concentrations on the system shown in the ESI.† As shown in curve a in Fig. S2A,† with the addition of 200 μM H_2O_2 into the buffer, a substantial increase in the CV response (curve b) appeared at the negative potential range that most likely reflected the onset of the peroxide reduction on this modified electrode compared with that without H_2O_2 (curve a). Fig. S2B† outlined the CV response of different concentrations of H_2O_2 on the system (Fig. S2B†). With the concentration of H_2O_2 increasing, the bioelectrocatalytic currents enlarged. The calibration curve corresponding to the CV responses of the modified electrode at different H_2O_2 concentrations was shown in the inset in Fig. S2B.† The response current was linear with the H_2O_2 concentration in the range, 20–200 μM, and the detection limit was 7 μM ($n = 3$).

3.4 Detection of DNA based on PB–Au nanocomposites and HRP-DNAzyme catalytic system

From a study of the optimal conditions shown in Fig. S3,† S2 was known to play an important role in the proposed biosensor. Thus, we could anticipate a quantitative nature for S2 based on the present system. Fig. 2A gave CV responses of S2 with varying concentrations on the present biosensor. Fig. 2B outlined the corresponding amperometric current curve. The electrochemical response linearly increased with the concentration of S2. The resulting calibration curve was shown in Fig. 2C. The electrocatalytic currents dynamically increased with the concentrations of S2 ranging from 0.15 to 0.95 μM with an achieved detection limit of 50 nM. A further aspect to consider is related to the specificity of the sensing platform and the possibility to discriminate base mismatches. As exhibited in Fig. 2D, the substitution of S2a (one base mismatch) or S2b (two bases mismatch) with S2 to fabricate the sensor had no

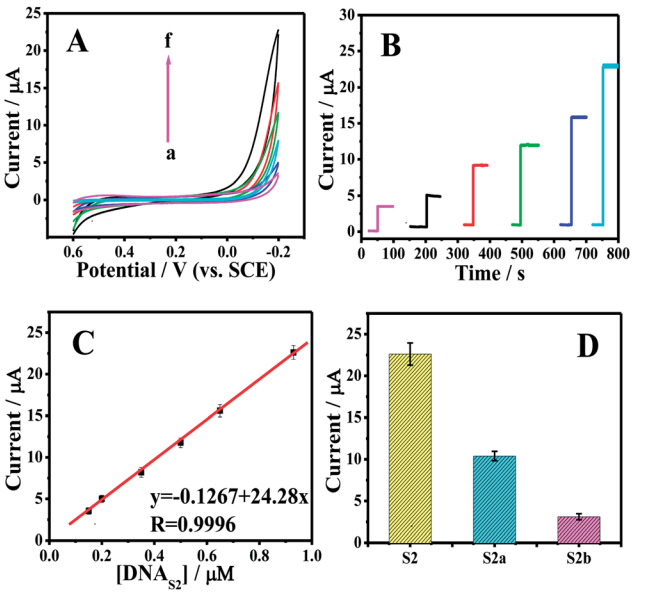

Fig. 2 (A) CV and (B) steady state amperometric current in 0.05 M PBS (pH 7.4) with 200 μM H_2O_2 on HRP-DNAzyme/S1/PB–Au/GCE incubated with various concentrations of S2 (a–f): 0.15; 0.2; 0.35; 0.5; 0.65; 0.95 μM; (C) corresponding calibration curve of biocatalytic reduction current *vs.* the concentration of S2; (D) selectivity of the HRP-DNAzyme/S1/PB–Au/GCE for S2 analysis in 0.05 M PBS (pH 7.4) with 200 μM H_2O_2.

significant effect on the electrochemical intensity, revealing the high selectivity of the proposed approach. Therefore, the proposed biosensor presented remarkably high sensitivity and selectivity.

3.5 Reproducibility and stability of the sensor

With only one step hybridization in the fabrication of the HRP-DNAzyme and PB–Au nanocomposites-modified GCE, good reproducibility of the modified electrode was obtained. A total number of six group DNA biosensors have been tested for its reproducibility. Each group was prepared under the same condition. The R.S.D.% of the response to the S2 of six different biosensors belonging to the same concentration was less than 6%. Besides the high sensitivity, selectivity and the reproducibility of this amplified electrochemical DNA sensor, we also tested its stability. After the biosensors were stored in a refrigerator for one week, 92.1% of the initial current response for DNA (0.95 μM as an example) could remain, indicating that the proposed method possessed acceptable stability.

3.6 Detection of Hg^{2+} based on PB–Au nanocomposites and HRP-DNAzyme catalytic system

The use of PB–Au and HRP-DNAzyme as platforms for amplified biosensing was further extended to develop selective Hg^{2+} ion sensors and aptasensors. Scheme 2 Part II depicts the configuration of the Hg^{2+} sensor that implements the PB–Au nanocomposites and HRP-DNAzyme. As we designed, S1 and S4 both had 9 thymine bases in their sequence. When the prepared S1/PB–Au/GCE was incubated in a PBS solution involving Hg^{2+}, S4 would hybridize with S1 by the T–Hg^{2+}–T base pairs. Meanwhile, in the presence of hemin and K^+, it could also result in the formation of the HRP-DNAzyme because the 5′ end of S4 was also a G-rich sequence, the same as that of S2. The Hg^{2+}–HRP-DNAzyme/S1/PB–Au/GCE was successfully fabricated. The electrocatalytic reduction of H_2O_2 by the HRP-DNAzyme provided a quantitative signal for the degree of the formation of the T–Hg^{2+}–T complex. Fig. 3A and B shows the CV data and the amperometric current responses with increasing concentrations of Hg^{2+} within the range from 10^{-10} to 10^{-2} M. The resulting calibration curve is outlined in Fig. 3C. The detection limit of 30 pM was then evaluated using a signal three-fold the background noise. Fig. 3D showed the selectivity of the sensor tested by substituting Hg^{2+} with various metal ions. The modified electrodes exhibited a remarkable peak current increase for Hg^{2+} but hardly responded to the other metal ions, indicating that the sensor had an impressive specificity toward Hg^{2+}. Such excellent selectivity should be ascribed to the specific T–Hg^{2+}–T coordination. This platform clearly showed the cooperative functions of the HRP-DNAzyme and the PB–Au nanocomposites in intensifying the current that enabled the ultrasensitive detection of the Hg^{2+} ions. In addition, the present detection system has the advantages of simplicity in design and easy operation over other recently developed electrochemical Hg^{2+} ions sensors (shown as Table S2†).

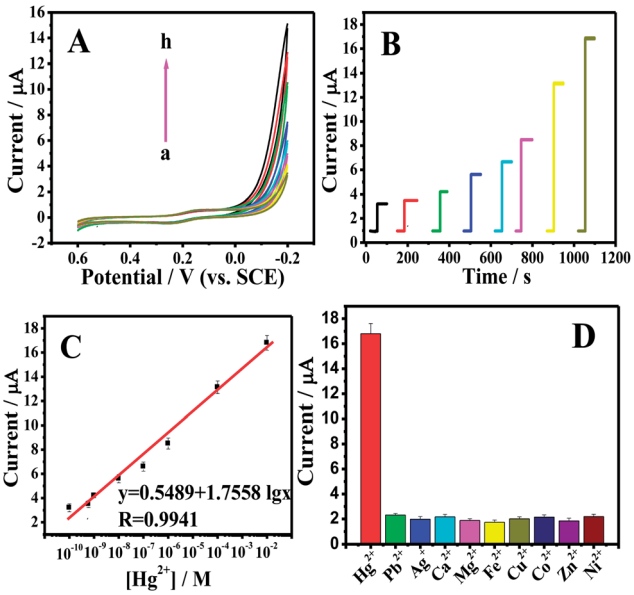

Fig. 3 (A) CV and (B) steady state amperometric current in 0.05 M PBS (pH 7.4) with 200 μM H_2O_2 on Hg^{2+}–HRP-DNAzyme/S1/PB–Au/GCE incubated with various concentrations of Hg^{2+} (a–h): 10^{-10}; 6×10^{-10}; 10^{-9}; 10^{-8}; 10^{-7}; 10^{-6}; 10^{-4}; 10^{-2} M; (C) corresponding calibration curve of the biocatalytic reduction current *vs.* the concentration of Hg^{2+}; (D) selectivity of the Hg^{2+}–HRP-DNAzyme/S1/PB–Au/GCE for Hg^{2+} analysis in 0.05 M PBS (pH 7.4) with 200 μM H_2O_2.

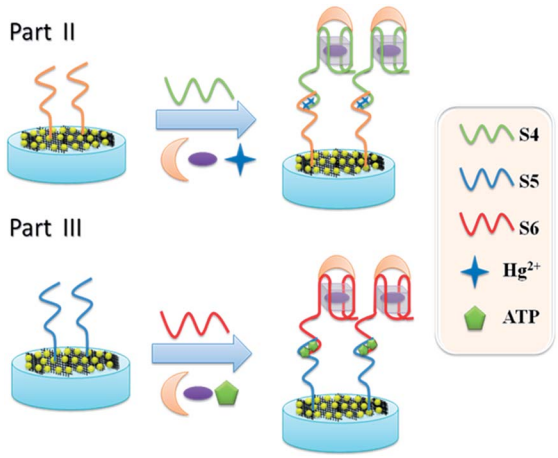

Scheme 2 Fabrication process of the electrochemical amplified determination of Hg^{2+} or ATP based on the PB–Au nanocomposite actuated HRP-DNAzyme system.

3.7 Detection of ATP based on PB–Au nanocomposites and HRP-DNAzyme catalytic system

Finally, the HRP-DNAzyme and PB–Au nanocomposites sensing platform was applied to detect ATP (Scheme 2 Part III). As shown in Scheme 2, S6 was designed with two sections. Section I was designed as a part of the ATP aptamer, and the sequence of section II was also a G-rich sequence, the same as that of S2, which could form HRP-DNAzyme in the presence of K^+ and hemin. S5 was the other part of the ATP aptamer. Thus, S6 could conjugate with S5 and ATP when incubated with S5/PB–Au/GCE

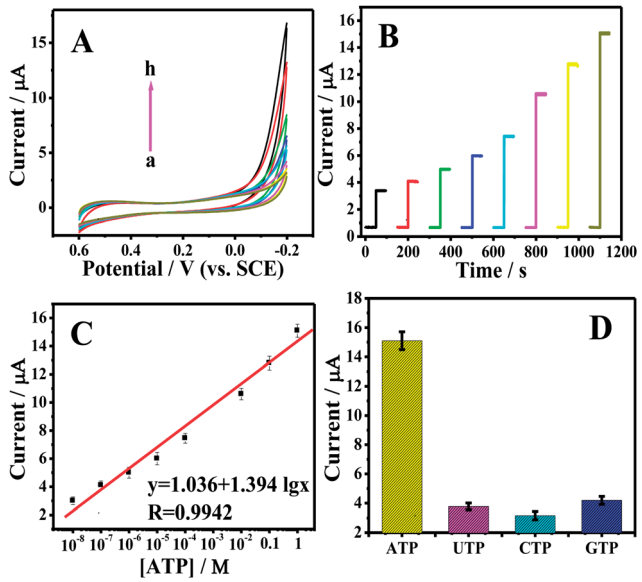

Fig. 4 (A) CV and (B) steady state amperometric current in 0.05 M PBS (pH 7.4) with 200 μM H_2O_2 on ATP–HRP-DNAzyme/S5/PB–Au/GCE incubated with various concentrations of ATP (a–h): 10^{-8}; 10^{-7}; 10^{-6}; 10^{-5}; 10^{-4}; 10^{-2}; 10^{-1}; 1 M; (C) corresponding calibration curve of biocatalytic reduction current *vs.* the concentration of ATP; (D) selectivity of ATP–HRP-DNAzyme/S5/PB–Au/GCE for ATP analysis in 0.05 M PBS (pH 7.4) with 200 μM H_2O_2.

and ATP to form ATP–HRP-DNAzyme/S5/PB–Au/GCE. The existence of ATP was the key to forming the resulting ATP–HRP-DNAzyme/S5/PB–Au/GCE. Fig. 4A and B showed the CV and amperometric current responses corresponding to different concentrations of ATP from 10^{-8} M on the ATP–HRP-DNAzyme/S5/PB–Au/GCE. Evidently, the analyte ATP could be detected at 10^{-8} M with a detection limit of 3 nM. The resulting calibration curve was depicted in Fig. 4C. The control experiments revealed no obvious changes upon guanosine triphosphate (GTP), uridine triphosphate (UTP), cytidine triphosphate (CTP) (equal concentration), as shown in Fig. 4D, which indicated that the sensing interface was selective for ATP due to the specific binding of ATP. In addition, this system is superior to other recently developed electrochemical ATP sensors in terms of sensitivity and selectivity (shown as Table S3†).

4. Conclusions

The present study introduced the PB–Au nanocomposites and HRP-DNAzyme in the versatile sensing platforms for the detection of DNA, ions, and aptamers. PB–Au nanocomposites and HRP-DNAzyme nanostructures constructed the catalytic cycling for signal amplification. Compared with the protein enzyme involved aptasensors, this new aptasensor possessed some advantages, such as without additional labelling, easy fabrication process involved only one-step hybridization and good stability against hydrolysis. More importantly, the use of PB–Au nanocomposites acting as a mediator stimulated the biocatalytic functions of HRP-DNAzyme for the development of the signal-amplified bioanalytical system. This novel electrocatalytical biosensor exhibited a wide linear range, low limit detection, and satisfactory operational stability. The highlight of this work was to adequately utilize the catalytic cycle of PB–Au nanocomposites and the use of the HRP-DNAzyme amplification platform for versatile sensing. It is expected that this electrochemical sensing platform will have many applications.

Acknowledgements

This work was financially supported by the projects (21073001, 21005001 and 21371007) from National Natural Science Foundation of China, Anhui Provincial Natural Science Foundation (1208085QB28), Anhui Provincial Natural Science Foundation for Distinguished Youth (1408085J03), Natural Science Foundation of Anhui (KJ2012A139) and the Program for Innovative Research Team at Anhui Normal University.

Notes and references

1 G. Pelossof, R. T. Vered, J. Elbaz and I. Willner, *Anal. Chem.*, 2010, **82**, 4396.
2 T. G. Drummond, M. G. Hill and J. K. Barton, *Nat. Biotechnol.*, 2003, **21**, 1192.
3 M. Campas and I. Katakis, *Trends Anal. Chem.*, 2004, **23**, 49.
4 F. A. Wang, J. Elbaz, C. Teller and I. Willner, *Angew. Chem., Int. Ed.*, 2011, **50**, 295.
5 M. M. Ali, S. D. Aguirre, H. Lazim and Y. F. Li, *Angew. Chem., Int. Ed.*, 2011, **50**, 3751.
6 C. W. Liu, C. C. Huang and H. T. Chang, *Anal. Chem.*, 2009, **81**, 2383.
7 B. Katz, B. Willner and I. Willner, *Nucleic Acid Protocols*, 2005, **1**, 195.
8 M. Tuomela, I. Stanescu and K. Krohn, *Gene Ther.*, 2005, **12**, 131.
9 G. A. Marko-Varga and P. L. Oroszlan, *J. Chromatogr. Libr.*, 2003, **68**, 1.
10 L. He, M. D. Musick, S. R. Nicewarner, F. G. Salinas, S. J. Benkovic, M. J. Natan and C. D. Keating, *J. Am. Chem. Soc.*, 2000, **122**, 9071.
11 D. J. Caruana and A. Heller, *J. Am. Chem. Soc.*, 1999, **121**, 769.
12 K. A. Edwards and A. Baeumner, *J. Anal. Chem.*, 2007, **79**, 1806.
13 U. Resch-Genger, M. Grabolle, S. Cavaliere-Jaricot, R. Nitschke and T. Nann, *Nat. Methods*, 2008, **5**, 763.
14 R. Polsky, R. Gill, L. Kaganovsky and I. Willner, *Anal. Chem.*, 2006, **78**, 2268.
15 B. Munge, G. D. Liu, G. Collins and J. Wang, *Anal. Chem.*, 2005, **77**, 4662.
16 G. Liu, Y. Wan, V. Gau, J. Zhang, L. H. Wang, S. P. Songand and C. H. Fan, *J. Am. Chem. Soc.*, 2008, **130**, 6820.
17 M. G. Zhang, A. Smith and W. Gorski, *Anal. Chem.*, 2004, **76**, 5045.
18 J. Zhao, Y. Y. Zhang, H. T. Li, Y. Q. Wen, X. Y. Fan, F. B. Lin, L. Tan and S. Z. Yao, *Biosens. Bioelectron.*, 2011, **26**, 2297.
19 X. B. Zhang, Z. Wang, H. Xing, Y. Xiang and Y. Lu, *Anal. Chem.*, 2010, **82**, 5005.

20 X. Tang, S. Bansaruntip, N. Nakayama, E. Yenilmez, Y. Chang and Q. Wang, *Nano Lett.*, 2006, **6**, 1632.
21 G. Pelossof, R. Tel-Vered, J. Elbaz and I. Willner, *Anal. Chem.*, 2010, **82**, 4396.
22 D. Li, B. Shlyahovsky, J. Elbaz and I. Willner, *J. Am. Chem. Soc.*, 2007, **129**, 5804.
23 Y. Weizmann, M. K. Beissenhirtz, Z. Cheglakov, R. Nowarski, M. Kotler and I. W. illner, *Angew. Chem., Int. Ed.*, 2006, **45**, 7384.
24 R. R. Breaker, *Nature*, 2004, **432**, 838.
25 P. J. Deuss, R. Den Heeten, W. Laan and P. C. Kamer, *Chem.–Eur. J.*, 2011, **17**, 4680.
26 X. H. Zhou, D. M. Kong and H. X. Shen, *Anal. Chem.*, 2010, **82**, 789.
27 A. X. Zheng, J. Li, J. R. Wang, X. R. Song, G. N. Chen and H. H. Yang, *Chem. Commun.*, 2012, **48**, 3112.
28 S. Bi, J. L. Zhang and S. S. Zhang, *Chem. Commun.*, 2010, **46**, 5509.
29 S. Bi, L. Li and S. S. Zhang, *Anal. Chem.*, 2010, **82**, 9447.
30 L. B. Zhang, J. B. Li, T. Zhu and E. K. Wang, *Anal. Chem.*, 2011, **83**, 8871.
31 Y. J. Song, Y. Chen, L. Y. Feng, J. S. Ren and X. G. Qu, *Chem. Commun.*, 2011, **47**, 4436.
32 Y. Weizmann, M. K. Beissenhirtz, Z. Che-glakov, R. Nowarski, M. Kotler and I. Willner, *Angew. Chem., Int. Ed.*, 2006, **118**, 7544.
33 C. Zhu, Y. Wen, D. Li, L. Wang, S. Song, C. Fan and I. Willner, *Chem.–Eur. J.*, 2009, **15**, 11898.
34 D. Li, A. Wieckowska and I. Willner, *Angew. Chem., Int. Ed.*, 2008, **120**, 3991.
35 T. Li, S. Dong and E. Wang, *Anal. Chem.*, 2009, **81**, 2144.
36 J. H. Chen, J. Zhang, Y. Guo, J. Li, F. F. Fu, H. H. Yang and G. N. Chen, *Chem. Commun.*, 2011, **47**, 8004.
37 L. Zhang, W. J. Gasper, S. A. Stass, O. B. Ioffe, M. A. Davis and A. J. Mixson, *Cancer Res.*, 2002, **62**, 5463.
38 T. Tatsuma, Y. Okawa and T. Watanabe, *Anal. Chem.*, 1989, **61**, 2352.
39 J. Ye and R. P. Baldwin, *Anal. Chem.*, 1988, **60**, 2473.
40 L. Gorton, A. Torstensson, H. Jaegfeldt and G. Jonsson, *J. Electroanal. Chem.*, 1984, **61**, 103.
41 Y. L. Yuan, G. P. Liu, R. Yuan, Y. Q. Chai, X. X. Gan and L. J. Bai, *Biosens. Bioelectron.*, 2013, **42**, 474.
42 G. Zhao, J. J. Feng, Q. L. Zhang, S. P. Li and H. Y. Chen, *Chem. Mater.*, 2005, **17**, 3154.
43 A. Walcarius, *Anal. Bioanal. Chem.*, 2010, **396**, 261.
44 S. S. Kumar, J. Joseph and P. K. Lakshminarasimha, *Chem. Mater.*, 2007, **19**, 4722.
45 Z. P. Zhang, A. Tang, S. Z. Liao, P. F. Chen, Z. Y. Wu, G. L. Shen and R. Q. Yu, *Biosens. Bioelectron.*, 2011, **26**, 3320–3324.
46 H. F. Chen, J. Tang, B. L. Su, G. N. Chen, J. X. Huang and D. P. Tang, *Anal. Chim. Acta*, 2010, **678**, 169.